The calorimetric spectrum of the electron-capture decay of ^{163}Ho. The spectral endpoint region

A. De Rújula^{a,b} **and M. Lusignoli**^{c}

^{a}*Instituto de Física Teórica, IFT-UAM/CSIC, Universidad Autónoma de Madrid,*
Campus de Cantoblanco, 28049 Madrid Spain

^{b}*CERN,*
1211 Geneva 23, Switzerland

^{c}*Sapienza, Università di Roma, and INFN — Sezione di Roma,*
Piazza A. Moro 2, I-00185 Roma, Italy

E-mail: Alvaro.DeRujula@cern.ch, maurizio.lusignoli@roma1.infn.it

ABSTRACT: The electron-neutrino mass (or masses and mixing angles) may be directly measurable in weak electron-capture decays. The favoured experimental technique is "calorimetric". The optimal nuclide is ^{163}Ho, and several experiments (ECHo, HOLMES and NuMECS) are currently studying its decay. The most relevant range of the calorimetric-energy spectrum extends for the last few hundred eV below its endpoint. It has not yet been well measured. We explore the theory, mainly in the cited range, of electron capture in ^{163}Ho decay. A so far neglected process turns out to be most relevant: electron-capture accompanied by the shake-off of a second electron. Our two main conclusions are very encouraging: the counting rate close to the endpoint may be more than an order of magnitude larger than previously expected; the "pile-up" problem may be significantly reduced.

Contents

1 Introduction

Fourscore and three years after Fermi computed how a nonzero neutrino mass would affect the endpoint of the electron spectrum in a β-decay process [1–3], the laboratory quest for a non-zero result in this kind of measurement is very much alive [4].

Weak electron capture (EC) has a sensitivity to the neutrino mass entirely analogous to the one of β-decay. EC is the $e\,p \to \nu\,n$ weak-interaction process whereby an atomic electron interacts with a nucleus of charge Z to produce a neutrino, leaving behind a nucleus of charge $Z - 1$ and a hole in the orbital of the daughter atom from which the electron was captured. The optimal nuclide in this respect is ^{163}Ho. The favoured experimental technique is "calorimetric" [5–7]. Various experiments — ECHo [8, 9], HOLMES [10] and NuMECS [11] — are currently making progress in this direction.

Once upon a time it was argued that the calorimetric energy spectrum of ^{163}Ho decay ought to be very well approximated by a simple theoretical expression: the sum over the Breit-Wigner-shaped contributions of the single holes left by electrons weakly captured by the nucleus [6]. In the extremely good approximation in which nuclear-size effects are neglected, the corresponding orbitals are the ones whose wave function at the origin is non-vanishing. In ^{163}Ho EC decay to ^{163}Dy the reaction's Q-value is smaller than the L (n=2) binding energies so that the potentially capturing orbitals (or resulting holes) are H = M1, M2, N1, N2, O1, O2 and P1, after which the 67th element (Ho) runs out of electrons.

Robertson has pointed out that two-hole contributions should not be negligible [12, 13]. In an EC event, the wave functions of the spectator electrons in the mother and daughter atoms are not identical, the small mismatch leading to an "instantaneous" creation of secondary holes, H'. An electron having been expelled from the H' orbital may be "shaken up" to an unoccupied atomic level or "shaken off" into the continuum. The ensuing contribution to the energy distribution would result in a peak for shake-up and a broad feature for shake-off.

The probabilities $P(\mathrm{H}, \mathrm{H}')$ for the production of two holes are much smaller than single-hole ones, $P(\mathrm{H})$. Yet, when the energy deficit of the two-hole state $E(\mathrm{H}, \mathrm{H}') \sim E(\mathrm{H}) + E(\mathrm{H}')$ is not very close to that of a prominent — but narrow — single-hole peak, there is an observable feature in the spectrum, even if $P(\mathrm{H}, \mathrm{H}') \ll P(\mathrm{H})$.

Robertson argues that *"If the presence of the curvature in the spectrum* [due to two-hole processes] *near the endpoint were not known to an analyst, fitting to the standard spectral shape would produce erroneous results for Q and m_ν"*. The two-hole processes, if significant, will be observed much before the analyst attempts to measure the cited parameters. Moreover, given the recently measured Q-value, $Q \equiv M(^{163}\mathrm{Ho}) - M(^{163}\mathrm{Dy}) = 2833\,(30_{\mathrm{stat}})\,(15_{\mathrm{sys}})$ eV [14], the dangerous possibility that $E(\mathrm{H}, \mathrm{H}') \sim Q$ for any given pair of holes is excluded.

The bad news is that the cited value of Q is larger than the previously "recommended" figure, $Q = 2.555 \pm 0.016$ keV [15], which goes in the direction of making a potential measurement of m_ν more difficult. The good news, as we shall argue, is that the contribution of two-hole states close to the spectral endpoint may compensate for the bad news, possibly in an overwhelming way.
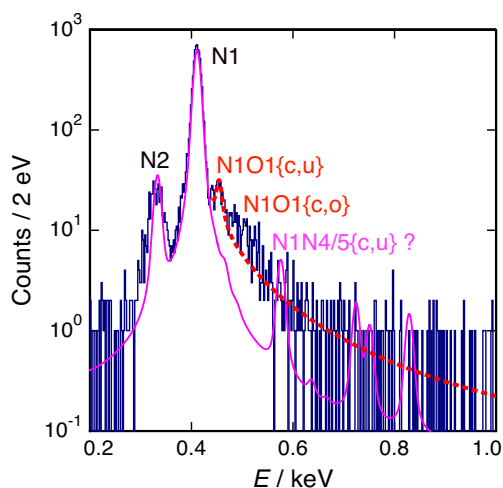
Figure 1. Blue: calorimetric spectrum measured by ECHo [16]. Magenta: prediction of Faessler et al. [19]. Red, dotted: added effect of the contributions N1O1{c,u} (arbitrarily multiplied by 2.5) and N1O1{c,o} [21]. The notation {c,u(o)} indicates that one electron is captured, one shaken up (off).

We shall be specifically interested in calorimetric energies, E_c, in a domain hardly explored so far, extending from the M1 peak at $E_c \sim 2050\,\mathrm{eV}$ to the endpoint at $E_c = Q - m_\nu$. Though QED and the weak-interaction theory are well established to impressive levels of precision, dealing with atoms containing up to 67 electrons is not entirely straightforward. Thus, we shall need observational input to guide our course.

2 Previous results

2.1 Data vs. theory

Some of the preliminary data of ECHo [16] (we thank L. Gastaldo for providing the figure to us) and NuMECS (we thank M. W. Rabin for providing the figure to us) are shown in figures 1, 2. There, they are compared with an elaborate theory of the calorimetric spectrum [17–19], smeared with the experimental resolution and with the inclusion of one, two and three-hole contributions. The agreement of theory and data is fairly good for the prominent M1, M2, N1 and N2 contributions.

There is in the ECHo data a significant peak at an energy close to the expected position of a contribution from N1 capture accompanied by O1 shakeup (N1O1), much larger than the theoretical expectation of [17–19]. There is no evidence, at the predicted level, for the contribution from N1 capture accompanied by N4/5 shakeup (N1N4/5) in either experiment. An expected, sizeable M1N4/5 peak is also apparently absent in the NuMECS data (it is tacitly assumed in these theoretical predictions [17–19] that the computed probability for the production of a second hole corresponds entirely to electron shakeup). Finally, in both data sets, there is evidence for a "shoulder" above the theoretical expectations in the $480\,\mathrm{eV} < E_c < 550\,\mathrm{eV}$ domain of calorimetric energy.

In [21] we have interpreted the situation just described in terms of a simple theory of the production of "second" holes, described in the following section. The predictions,
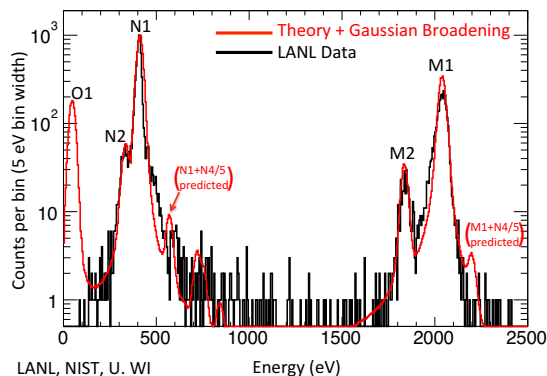
Figure 2. Black: calorimetric spectrum measured by NuMECS. Red: theoretical prediction of Faessler et al. [19].
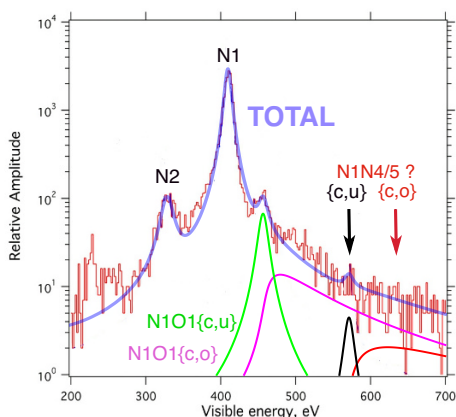

Figure 3. The N-region. Slightly doctored predictions from [21], compared with early ECHo data, as reported in [12]. The excess below 300 eV is due to a ^{144}Pm contamination. The resolution's width (FWHM) is taken to be $\Delta E_{\text{exp}} = 8.4\,\text{eV}$.

for the region close to the N1, N2 single-hole peaks, are shown in figure 3. In this and subsequent figures, the symbols {c,u} and {c,o} refer to one electron being captured (c), the other one being shaken up (u) or off (o). The curly brackets remind us that the electrons are indistinguishable and their wave functions anti-symmetrized.

Once again, theory [21] and data disagree. Our estimate of the height of the N1O1{c,u} shakeup peak is a factor ~ 2.5 too low. It is possible to correct in similarly moderate ways the other contributions such as to agree with the data. One possibility, illustrated in figure 3, is to correct the N1O1{c,u} peak by the cited factor and to leave N1O1{c,o} shake-off shoulder — which snugly describes the observed one — as predicted, while reducing the N1N4/5 features by a factor ~ 3.

2.2 Lessons

We conclude from the comparison of theory and preliminary data that the predictions for the subdominant spectral features due to the production of more than one hole are to be taken *cum amplo grano salis*.

As we wall discuss in more detail in sections 6 and 9, it is not a surprise that the precise positions, heights and widths of the single- and multiple-hole contributions ought to be fit to the observations. Only the Breit-Wigner shape of a single peak (or shakeup multiple peak) is theoretically hale and hearty. Much less so is the shape of a shakeoff feature which, computed in the customary sudden approximation, depends on an overlap of bound and unbound wave functions.

Finally, the predictions for the normalization of the various contributions, particularly the more elaborate ones [17–19], seem to be very untrustworthy. On the way to an analysis of the endpoint, the size of the various spectral features will need to be adjusted to fit the data. Currently, there are no theoretical results for the shake-off contributions, akin to those of [17–19] for the shake-up probabilities. It would be useful to know whether the shapes of these shake-off contributions agree with those of our more naive approach which, as we have seen, agree with the preliminary data.

3 A rough theoretical guidance

In this section we clone the simple theory of the production of one [6] or more holes [21] in electron capture, adapting it to the region of calorimetric energies extending from the M1 and M2 holes to the spectral endpoint.

3.1 The spectrum of single holes

In its simplest approximation [6] the spectrum of calorimetric energies, E_c, is a sum of Breit-Wigner (BW) peaks at the $E_c = E_H$ positions,[1] with their natural hole widths, Γ_H. The peak intensities are proportional to $\phi_H^2(0)$, the values in Ho of the squared wave functions at the origin of the electrons to be captured. The contribution of a single hole to the EC decay rate, R, as a function of E_c is:

$$\frac{dR[\mathrm{H}]}{dE_c} = \kappa\, E_\nu\, p_\nu\, n_H\, \phi_H^2(0)\, BW[E_c, E_H, \Gamma_H], \tag{3.1}$$

$$BW[E_c, E_H, \Gamma_H] \equiv \frac{\Gamma_H}{2\pi} \frac{1}{(E_c - E_H)^2 + \Gamma_H^2/4}, \tag{3.2}$$

$$E_\nu = (Q - E_c), \qquad p_\nu = \sqrt{(Q - E_c)^2 - m_\nu^2}, \tag{3.3}$$

The factor E_ν in eq. (3.1) originates from the (squared) weak-interaction matrix element and the factor p_ν in the decay's phase space. Having made explicit the E_ν factor, κ — in the excellent approximation in which nuclear recoil is neglected — is a constant:

$$\kappa\, E_\nu \equiv \frac{G_F^2}{4\pi^2} \cos^2\theta_C\, B_H\, |\mathcal{M}|^2, \tag{3.4}$$

with $\mathcal{M}$ the nuclear matrix element, $B_H - 1$ [20] an $\mathcal{O}(10\%)$ correction for atomic exchange and overlap and n_H the electron occupancy in the H shell of Ho (the actual fraction of the maximum number of electrons with the quantum numbers of H).

---

[1]The daughter Dy* atom has a hole and an extra electron in the N7 ($4f_{7/2}$) level, of binding energy $\sim 4.2\,\mathrm{eV}$, so that, more precisely, $E_c = E_H - E_{N7}$. We do not in the text make this small correction. In comparisons with data the predictions for the peak positions will anyway be slightly adjusted to fit.

We know from the observations of neutrino oscillations that the electron neutrino is, to a good approximation, a superposition of three mass eigenstates, ν_i: $\nu_e = \sum_i U_{ei}\nu_i$, with $\sum_i |U_{ei}|^2 = 1$. Thus, we ought to have written $dR[\mathrm{H}]/dE_c$ in eqs. (3.1)–(3.4) as an incoherent superposition of spectra with weights $|U_{ei}|^2$ and masses $m(\nu_i)$. But the measured differences $m^2(\nu_i) - m^2(\nu_j)$ are so small that the sensitivity of current direct attempts to measure m_ν may result in a positive result only if neutrinos are nearly degenerate in mass, in which case m_ν in eqs. (3.1)–(3.4) stands for their nearly common mass.[2]

We have, in eq. (3.1), made the "classical" approximation of neglecting interferences between different vacated orbitals. For two different intermediate states H and H' to interfere, it is necessary that they decay into the same subsequent state. The probability for this to happen, in the case we are discussing, is small. An estimate of a generous upper limit to the effect of interferences is discussed in appendix A, demonstrating that interferences may be neglected.

3.2   Shake-up

As Robertson pointed out [12, 13], in an EC event leading to a primary hole H there is a small probability for a second hole H' to be made in a shake-up process. When the second electron is shaken-up to any unoccupied daughter-atom bound-state level — of binding energy negligible relative to $E_{\mathrm{Tot}} \sim E(\mathrm{H}) + E(\mathrm{H}')$ — the calorimetric energy has a peak at $E_c \sim E_{\mathrm{Tot}}$.

To the extent that the presence of one hole does not significantly affect the filling — i.e. decay — of the other, the natural width of a two-hole state is the sum of the partial widths: $\Gamma_{\mathrm{Tot}} \simeq \Gamma(\mathrm{H}) + \Gamma(\mathrm{H}')$. In analogy to the one-hole result of eqs. (3.1)–(3.4), the contribution of a particular two-hole state to the calorimetric spectrum is:

$$\frac{dR[\mathrm{H},\mathrm{H}']}{dE_c} = \kappa \ E_\nu \, p_\nu \, n_{\mathrm{H}} \, n_{\mathrm{H}'} \, BW[E_c, E_{\mathrm{Tot}}, \Gamma_{\mathrm{Tot}}] \sum_{n=7}^{\infty} |\{1 - \Pi(\mathrm{H},\mathrm{H}')\}\phi_{\mathrm{H}}(0) \, A(\mathrm{H},\mathrm{H}',\mathrm{n})|^2,$$

(3.5)

where $n_{\mathrm{H}'}$ is the occupancy in the H' shell, $\phi_{\mathrm{H}}(0)$ is the wave function at the origin of the captured electron, $A(\mathrm{H},\mathrm{H}',\mathrm{n})$ is the probability amplitude for the excitation of the electron in H' to an unoccupied S-wave bound state with n its principal quantum number,[3] and $\Pi(\mathrm{H},\mathrm{H}')$ is the operator interchanging the two implicated electrons. More precisely, $1 - \Pi(\mathrm{H},\mathrm{H}')$ stands for the operation of symmetrizing the product of captured wave function and transition amplitude in the singlet antisymmetric spin state, antisymmetrizing it in the triplet symmetric spin state and adding the resulting square moduli with weights $1/4$ and $3/4$.

3.3   Shake-off

The creation of a second hole H' in the capture leaving a hole H can also occur as the shake-off of the electron in the orbital H' to the "continuum" of unbound electrons:

$$\mathrm{Ho} \to \mathrm{Dy}[\mathrm{H},\mathrm{H}'] + e^- + \nu_e. \tag{3.6}$$

---

[2]If there were a small mixture of an extra mass eigenstate, it could be seen as a kink in the spectrum [22, 23].

[3]In the particular case of (H, H') = (M1, N1) one would have $A(\mathrm{H},\mathrm{H}',\mathrm{n}) = B_n$, as defined and estimated in eq. (3.13).

In such a 3-body decay, neither the electron nor the neutrino are approximately monochromatic. The neutrino energy, E_ν, and the ejected electron's kinetic energy, T_e, satisfy $E_\nu + T_e = Q - E_{\text{Tot}}$. The electron's energy and the daughter Dy ion energy excess add up to the observable calorimetric energy $E_c = T_e + E_{\text{Tot}}$.

Let $|\text{Ho}[\text{H}]\rangle$ be the wave function, in Ho, of the orbital whose electron is to be captured and $|\text{Dy}[\text{H}, \text{H}'; p_e]\rangle$ the continuum wave function of the electron ejected off the daughter two-hole Dy ion. In the sudden limit the shakeoff distribution in electron momentum p_e (or in its energy T_e) ensues from the square of the wave function overlap:

$$\frac{dM}{dp_e} \equiv |\{1 - \Pi(\text{H}, \text{H}')\}\, \phi_{\text{H}}(0)\, \langle \text{Ho}[\text{H}']|\text{Dy}[\text{H}, \text{H}'; \text{p}_{\text{e}}]\rangle|^2, \tag{3.7}$$

$$\frac{dM}{dT_e} = \frac{m_e}{p_e} \frac{dM}{dp_e}, \tag{3.8}$$

where we have defined the auxiliary function dM/dp_e, to be used anon.

It is simplest to discuss the rate for the shake-off process of eq. (3.6) by doing it for starters in the vanishing-width approximation for the daughter holes. In this case

$$\frac{dR}{dT_e} = \kappa\, E_\nu\, p_\nu\, n_{\text{H}}\, n_{\text{H}'}\, \frac{p_e}{4\pi^2} \frac{dM}{dT_e}. \tag{3.9}$$

The resulting E_c distribution is:

$$\frac{dR}{dE_c} = \int_0^{Q-E_{\text{Tot}}} \frac{dR}{dT_e}\, \delta(E_c - E_{\text{Tot}} - T_e)\, dT_e. \tag{3.10}$$

To undo the zero-width approximation, substitute the above δ function by $BW[E_c - T_e, E_{\text{Tot}}, \Gamma_{\text{Tot}}]$, with BW defined as in eq. (3.2).

3.4 The shake-off shape

Electron capture in Ho results in a Dy atom — which we shall in what follows denote as Dy* — with a hole in the orbital from which the capture took place. The absent-electron charge partially shields the one of the absent-proton. Relative to a process without a similar effect — such as the creation of a primary hole by photo-ionization — the partial shielding generally leads to a reduced probability for the creation of a second hole. This is because the wave functions of the potentially vacated second orbitals in the parent and daughter atoms have a closer overlap in the presence of shielding. And — in the sudden approximation traditionally used to make these kind of estimates — the square of this overlap is the probability of not creating a second hole.

Intemann and Pollock [24] were the first to show how to properly treat the shake-off of a second electron in EC. In what follows we apply their method and refer as an example to M1 capture accompanied by N1 shakeoff, or, more precisely, to the M1N1{c,o} process (the most relevant one closest to the spectral endpoint). The trick is to start by treating the result of M1 capture (the absent proton and the absent electron) as a perturbation of the Coulomb potential of the form:

$$\alpha\, b(r) \equiv \alpha \left(\frac{1}{r} - \int d^3 r_1\, \frac{|\phi_{\text{M1}}(r_1)|^2}{|\vec{r} - \vec{r}_1|} \right). \tag{3.11}$$

To first order in α the wave function of the N1 level in Dy* (the daughter atom with an M1 hole) is then expressed as a linear combination of Ho eigenfunctions:

$$|\text{Dy}^*[\text{N1}]\rangle \simeq |\text{Ho}[\text{N1}]\rangle + \sum_n B_n \, |\text{Ho}[n]\rangle + \frac{1}{2\,\pi} \int_0^\infty dp_e \, B_{\text{off}}(p_e) \, |\text{Ho}[p_e]\rangle, \tag{3.12}$$

$$B_n \equiv \frac{\alpha}{E_{\text{N1}} - E_n} \int d^3r \, \phi_n^*(r) \phi_{\text{N1}}(r) \, b(r), \tag{3.13}$$

$$B_{\text{off}}(p_e) \equiv \frac{\alpha}{E_{\text{N1}} + T_e} \int d^3r \, \phi^*(p_e, r) \phi_{\text{N1}}(r) \, b(r) \tag{3.14}$$

where n in the wave functions $|\text{Ho}[n]\rangle$ stands for the $l = 0$ bound levels with $n \neq 4$ and (positive) binding energy E_n, $\phi(p_e, r)$ is the unbound wave function of the state $|\text{Ho}[p_e]\rangle$, defined as in [25], of an $l = 0$ electron with momentum p_e and kinetic energy $T_e = p_e^2/(2\,m_e)$.

To take into account Fermi statistics, one must — it goes without saying — also do the calculations encapsulated in eqs. (3.11)–(3.14) with the exchange M1 $\leftrightarrow$ N1, since the two-hole final state, at a given T_e, is the same independently of which electron is captured or ejected. Thus, in the sudden approximation, the square of the (monopolar) matrix element for an electron being shaken-off with energy T_e results in:

$$\frac{dM}{dT_e} = \frac{m_e}{4\,\pi^2\,p_e} \left|\{1 - \Pi(\text{M1}, \text{N1})\} \, \phi_{\text{M1}}(0) B_{\text{off}}(p_e)\right|^2 \tag{3.15}$$

for the distribution function of eq. (3.8).

A crucial point in estimating wave-function overlaps is to choose them with the correct spatial scale. To provide an estimate of the shape of dM/dT_e we shall use non-relativistic Coulomb wave functions[4] of Ho with effective values of Z chosen to reproduce the relevant orbits' mean radii, as calculated with more precise Hartree-Fock methods [26]. Let $r_B \equiv 1/(\alpha\,m_e)$ denote the Bohr radius. For $\langle r(\text{M1}) \rangle = 0.246\,r_B$ and $\langle r(\text{N1}) \rangle = 0.555\,r_B$ the effective charges are $Z_{\text{eff}}(\text{M1}) = 54.9$, to be used in eq. (3.11) and $Z_{\text{eff}}(\text{N1}) = 43.2$, to be used for the bound and free wave functions in eqs. (3.13), (3.14).

4 The M-hole region and beyond

In what follows we present results for the spectral domain extending from the M2 and M1 single-hole contributions to the spectral endpoint, assumed to be at Q = 2833 keV. First we take at face value the results of the calculations described in the previous section. Since the results are very optimistic — in the sense of facilitating a potential constraint on m_ν — we shall later discuss the possibility that our predictions are gross overestimates.

In figure 4 we show the separate contributions of the one-hole spectrum, the dominant contribution to the two-hole spectrum in this energy domain (M2H plus M1H), and the one-plus-two-hole result.[5] This is a *theorist's spectrum*, with an arbitrarily normalized vertical

---

[4]These would give very poor estimates of the wave functions at the origin, for which we use instead the values given by the accurate calculations in [13, 17–19].

[5]We did not include other two-hole contributions (like N1M4 and N1M5) giving small structures below the M2 peak.
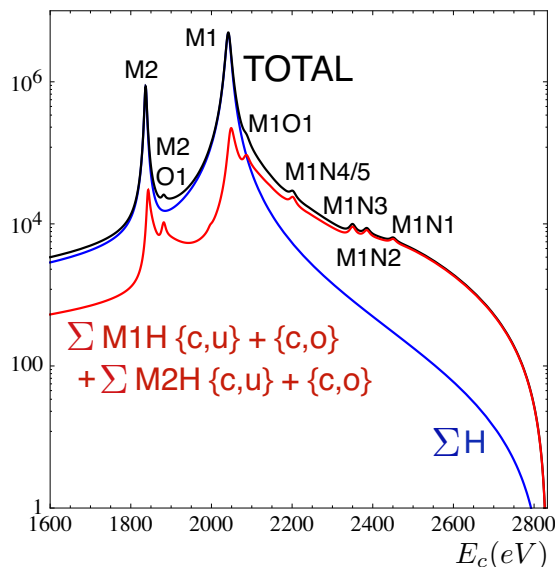
Figure 4. The "theorist's" calorimetric spectrum in the M region. In blue the single-hole contribution ΣH. In red the two-hole shake-up plus shake-off contributions, with one of the holes being M1 or M2. In black, the sum of all contributions. The units of the vertical scale are arbitrary.

scale, $m_\nu = 0$ and an experimental width, $\Delta E_{\exp}$, whose square is negligible relative to that of any of the hole's natural widths. All the subsequent figures will also, in the same sense, depict arbitrarily normalized spectral shapes, occasionally with $m_\nu \neq 0$.

The enhancement above the M1 peak of the total spectrum in figure 4, relative to the single-hole result, is quite considerable. A very good way to present this phenomenon is to plot the *bare spectrum*, i.e. the result of dividing the numbers of events of figure 4, by $E_\nu \, p_\nu$, the factors originating from the nuclear matrix element and the phase space, respectively. This is done in figure 5. In this and subsequent plots of "bare spectra" the vertical scale is arbitrary and we do not even label it.

Notice in figure 5 that, at $E_c \sim Q$, the two-hole contributions are overwhelmingly dominant, a factor ~ 40 larger than the single-hole contribution.[6] In a closer look at the figure one concludes that this large effect would be equivalent, in the absence of two-hole contributions, to a Q-value of $\sim 2150\,\mathrm{eV}$, a point of the green single-hole curve with an ordinate as high as the endpoint of the (total) blue curve.

An analogous improvement is expected on another subject: the possible observation of antineutrinos of the cosmic background via their capture in ^{163}Ho. The quantity of radioactive isotope necessary to obtain ten events of signal is a strongly increasing function of the Q-value [29]: with only single-hole EC it should be 1274 (23.2) kg y for Q = 2.8 (2.2) keV. Including the contribution to the two-hole spectrum the same quantity comes out to be 30.6 kg y even if Q = 2.833 keV. Gathering this amount of ^{163}Ho is still a wee bit unrealistic.

---

[6]The figure is plotted for a fixed height of the M1 peak. With this constraint, the NH and MH contributions increase the overall normalization of the spectrum by $\sim 9\%$, so that, for a fixed total number of events, the enhancement would be closer to 40 than to 43, should we trust the double-hole predictions to this level of precision.
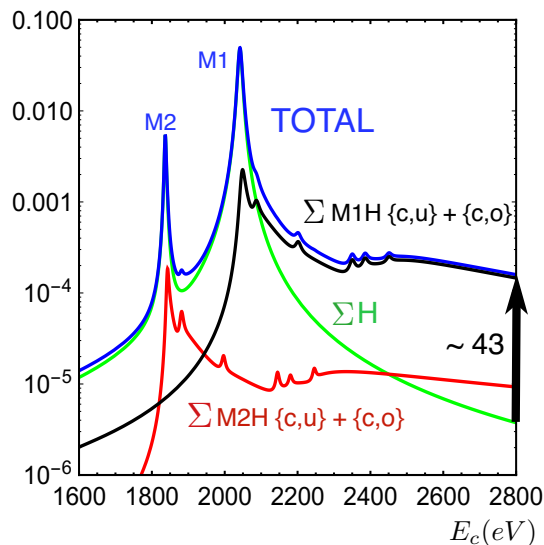
Figure 5. The "bare" spectrum defined in the text. The normalization of the ordinate is arbitrary. In black (red) the sum of the two-hole spectrum, one of the holes being M1 (M2). In green, the single-hole contribution. In dark blue, the total. The units of the vertical scale are arbitrary.
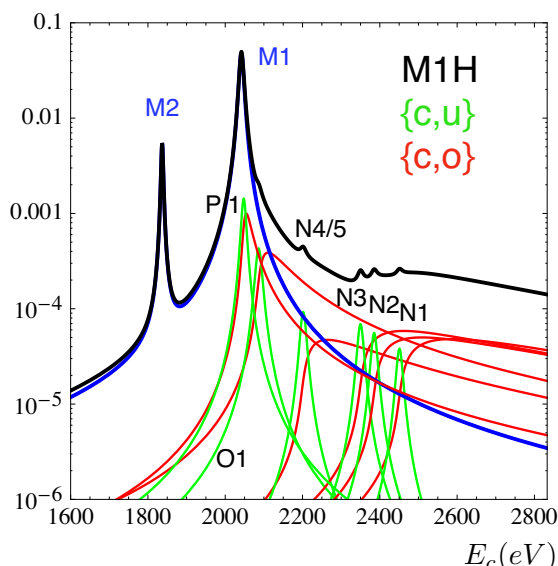

Figure 6. The M1H two-hole contributions in figure 5, in full detail. In green (red), one of the holes is captured, the other one shaken up (off). In black a total bare spectral shape, including the (blue) single-hole contribution, but not the M2H contributions, negligible above the M1 peak. The units of the vertical scale are arbitrary.

The details contributing to the construction of figure 5 are given in figures 6, 7, where, respectively, the various M1H and M2H double-hole contributions are specified.

We have seen that some two-hole effects successfully compete with single-hole ones when the sizable contribution of the former is at E_c values at which the latter is not close to its peak. The triple-hole contributions, contrariwise, are largest at E_c values at which the shake-off contribution of double holes is relatively large. Given the smallness of the extra
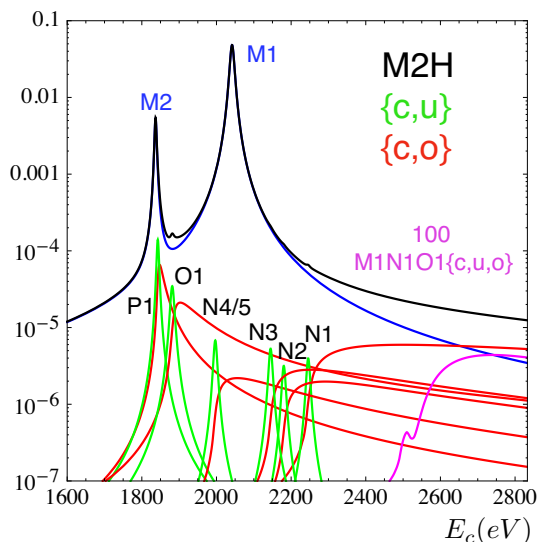
Figure 7. The M2H two-hole contributions in detail. In green (red), one of the holes is captured, the other one shaken up (off). In black a total bare spectrum including the (blue) single-hole contribution, but — unrealistically — not the M1H contribution. Enhanced by two orders of magnitude, the M1N1O1{c,u,o} three-hole contribution is also shown. The units of the vertical scale are arbitrary.

wave-function overlap in three-hole contributions (relative to the two-hole ones), three-hole effects are always negligible. The example of M1N1O1{c,u,o}, arbitrarily multiplied by a factor of one hundred, is shown in figure 7.

5   The endpoint analysis

The spectral shape in the last $\sim 700\,\mathrm{eV}$ below the endpoint is shown in the upper figure 8, where the dominance of double-hole contributions is predicted to be most significant. The lower figure is a "Kurie" (or Kurie-like plot), simply depicting the square root of the number of (theorist's) "events". Notice that in the last $200\,\mathrm{eV}$, there being no significant spectral features (double hole {c,u} peaks or {c,o} thresholds) the Kurie plot is linear but, as we proceed to discuss, not quite. Recall here, and in what follows, that we have assumed that our "experiment" has a perfect resolution.

The uppermost $\sim 200\,(30)\,\mathrm{eV}$ of the Kurie plot are shown in the upper (lower) part of figure 9. We are only interested in checking the degree of non-linearity of this theoretical plot, so our disrespect for statistical issues will be irrelevant. Our theorists' "Kurie data", generated with $m_\nu = 0$, $Q = 2833\,\mathrm{eV}$, are fit to a linear and a quadratic polynomial in E_c, in a theorist's way. To wit, the interval $Q-200 \leq E_c \leq Q-2\,\mathrm{eV}$ (or Q - 10 eV, to check that the a-priori ignorance of a precise calorimetric Q-value makes little difference) is binned in ~ 100 2-eV intervals. Two least square fits to this binned "data" are performed, ignoring the fact that, in reality, the real data would be statistically more precise as E_c decreases.

The results of the fits are:

$$\mathrm{A}(E_c) = 51.9226 - 0.018363 E_c, \tag{5.1}$$

$$\mathrm{B}(E_c) = 162.652 - 0.0994605 E_c + 1.4842\,10^{-5} E_c^2. \tag{5.2}$$
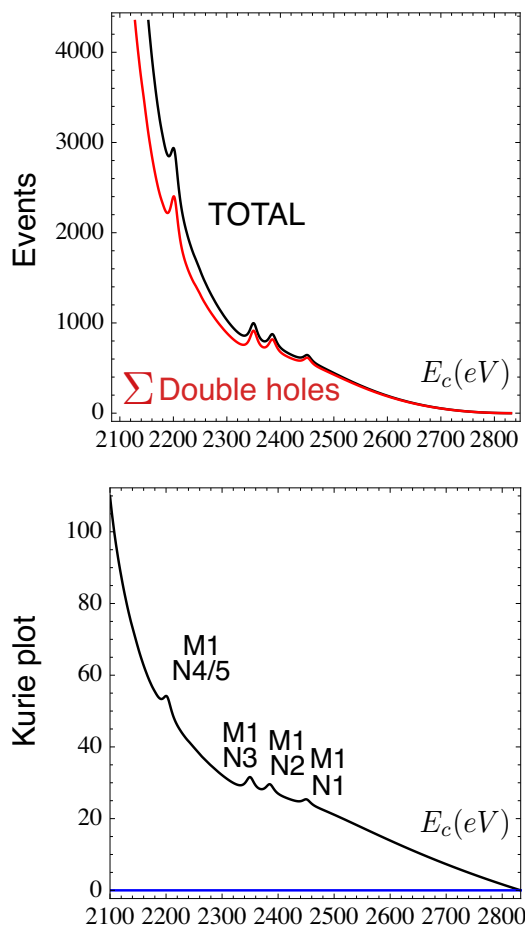
Figure 8. *Above*: the uppermost $\sim 700\,\mathrm{eV}$ of the spectrum, with an arbitrary vertical scale. *Below*: the corresponding Kurie plot (the square root of above-plotted spectral shape).

The linear fit is not very good, while the quadratic one very snugly describes the "data". The condition $A(E_c) = 0$ results in $Q = 2827.56\,\mathrm{eV}$, wrong by $\sim 0.19\%$ relative to the "data's" $Q = 2833\,\mathrm{eV}$. The condition $B(E_c) = 0$ results in $Q = 2833.14\,\mathrm{eV}$, correct to 5 parts in 10^5.

In the lower part of figure 9 we test "by eye" how the mentioned "Kurie data" or the linear and quadratic fits thereof would, given the required statistics and the other obvious provisos, exclude neutrino masses of 2 or 5 eV.

6 An evident caveat

We have been treating our predictions as if they were to be precisely trusted. But we have seen, by comparing them with the preliminary data in the N-region of energies, that they are not. The theory appears to overestimate some double hole contributions, and to underestimate others. Moreover our results about the analysis of the endpoint appear to be unprecedently optimistic, and this will be even more so when we discuss the pile-up issue. Thus, we adopt in this section a complementary very pessimistic point of view.
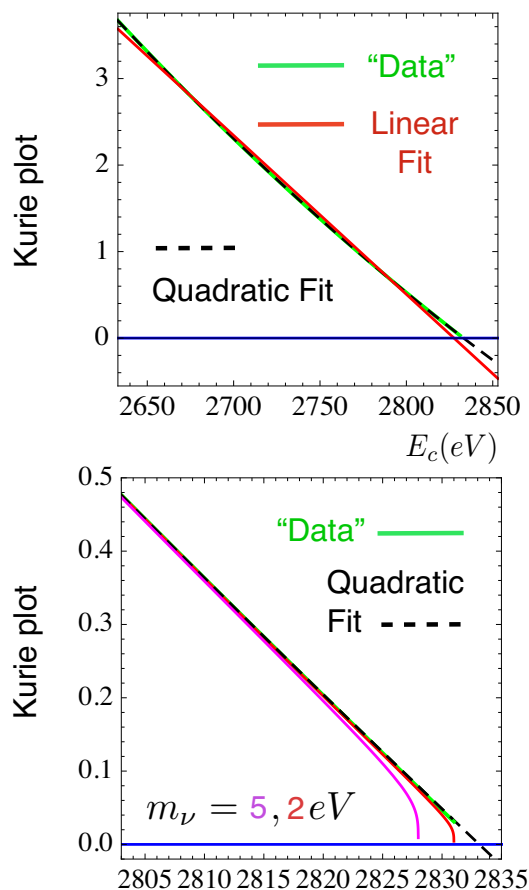
Figure 9. *Above*: the uppermost $\sim 200\,\mathrm{eV}$ of the Kurie plot, showing a linear and a quadratic fit to the theoretical $Q = 2833\,\mathrm{eV}$, $m_\nu = 0$ "data". *Below*: the last $\sim 30\,\mathrm{eV}$, including the expectations for $m_\nu = 2, 5\,\mathrm{eV}$, which disagree with the input "data".
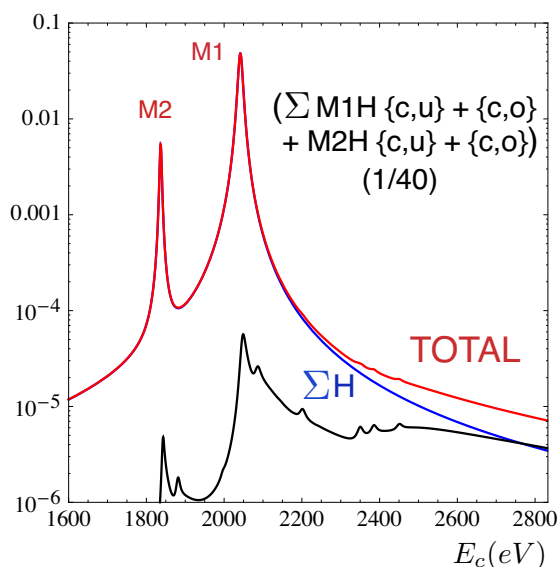

Figure 10. Bare spectrum with all double-hole contributions arbitrarily divided by 40, with their sum in black. Blue: the sum of single holes. Red: total.
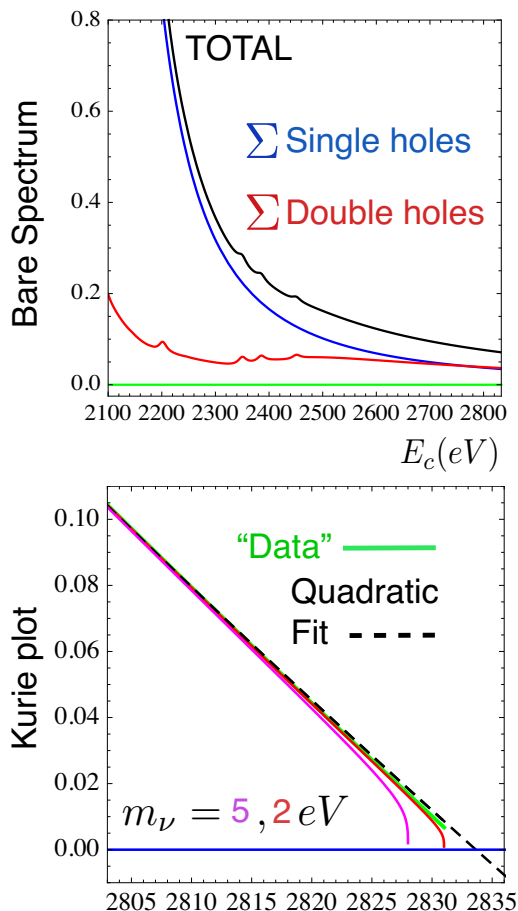
– 13 –

Figure 11. *Above*: bare spectrum of the uppermost $\sim 700\,\mathrm{eV}$ of an $m_\nu = 0$ set of "data" with the predicted two-hole contributions arbitrarily diminished by a factor of 40. *Below*: the corresponding Kurie plot in the last $30\,\mathrm{eV}$, showing also a linear and a quadratic fit, as well the theoretically excludable expectations for $m_\nu = 2, 5\,\mathrm{eV}$.

Assume that all the double hole contributions relevant to the endpoint analysis (M1H and M2H) have been overestimated by a collective factor of 40, chosen to have their sum at $E_c \sim Q$ be comparable to the M1-dominated single hole contribution in that domain. The corresponding bare spectral shapes are shown in figure 10.

In the upper part of figure 11 we show the bare spectrum, at energies above $Q - 700\,\mathrm{eV}$. The lower part is the corresponding Kurie plot, showing a quadratic fit to the "data" analogous to that described in connection with the lower part of figure 9.

Once again, we make linear and quadratic fits to the "data", binned in the last $\sim 200\,\mathrm{eV}$ below the endpoint. The results are:

$$\mathrm{A}'(E_c) = 11.9492 - 0.0042288\,E_c, \tag{6.1}$$

$$\mathrm{B}'(E_c) = 47.8908 - 0.0305521\,E_c + 4.81759\,10^{-6}\,E_c^2. \tag{6.2}$$

The linear fit is not very good, while the quadratic one very snugly describes the "data". The condition $\mathrm{A}'(E_c) = 0$ results in $Q = 2825.67\,\mathrm{eV}$, wrong by $\sim 0.26\%$ relative

to the "data's" $Q = 2833\,\text{eV}$. The condition $B'(E_c) = 0$ results in $Q = 2833.65\,\text{eV}$, correct to 2.3 parts in 10^4.

6.1 A preliminary conclusion

Assume that, in a particular experiment, the experimental resolution function and the background are well understood. Traditionally, Kurie plots for well understood processes — such as tritium β-decay — are defined in such a way that they are expected to be linear in energy. They are then fit with three parameters: m_ν and the constant and the slope of a linear function of energy or, equivalently, m_ν, the slope and Q.

In the case of the calorimetric measurement in ^{163}Ho EC the shape of the BW functions describing single-hole or HH'{c,u} double-hole contributions, as we shall discuss, are very well understood. The "problem" is that the precise shape and magnitude of the HH'{c,o} double-hole contributions are not. Even if these contributions are measured to be significant as one approaches the endpoint, we have argued, the use of one more parameter in the fits (the extra coefficient in a quadratic function of energy) should solve this apparent problem.

It goes without saying that these theoretical conclusions would gain (or lose) weight if and when they are tested with adequate simulations of data in a realistic observational environment. The advantages of a possibly increased statistics in the endpoint region (compared with single-hole expectations) may be a tempting reason to perform such an analysis.

7 Pile-up

The finite time required to record an EC event gives rise to the inescapable problem of pile-up: the additional contribution of the spectrum of two "simultaneous" events. If the "singles" spectrum (of single events) has a sizable contribution of HH'{c,o} events towards its endpoint, the concern with pile-up *diminishes*.

Let $d\hat{R}/dE_c$ be the singles spectrum, with its integral in the interval $0 < E_c < Q$ normalized to unity. The pileup spectrum, also normalized to unity in the interval $0 < E_c < 2\,Q$, is:

$$\frac{dR_P}{dE_c} = \int_0^Q dE_1 \int_0^Q dE_2 \, \frac{d\hat{R}}{dE_1} \frac{d\hat{R}}{dE_2} \, \delta(E_c - E_1 - E_2). \tag{7.1}$$

For the sake of illustration, let the probability of pileup be 4×10^{-5}. In the upper part of figure 12 we show the corresponding singles and pileup spectra for the case in which they are exclusively dominated by single-hole captures; the vertical scale is arbitrary, but the ratio of the two spectra is not, it corresponds to the assumed energy-integrated pileup probability. With the same proviso,[7] the spectra corresponding to our estimate of two-hole effects are shown in the lower part of figure 12.

Comparing the emphasized regions in the upper and lower parts of figure 12 one concludes that the end-point pileup problem is much less serious in the case that the double-hole contributions are significant there. This is made clearer by comparing the

---

[7]A hawk-eyed reader may notice that these spectra do not have the little wiggles visible in figure 4. They have been smoothed in the benefit of a faster numerical integration of eq. (7.1).
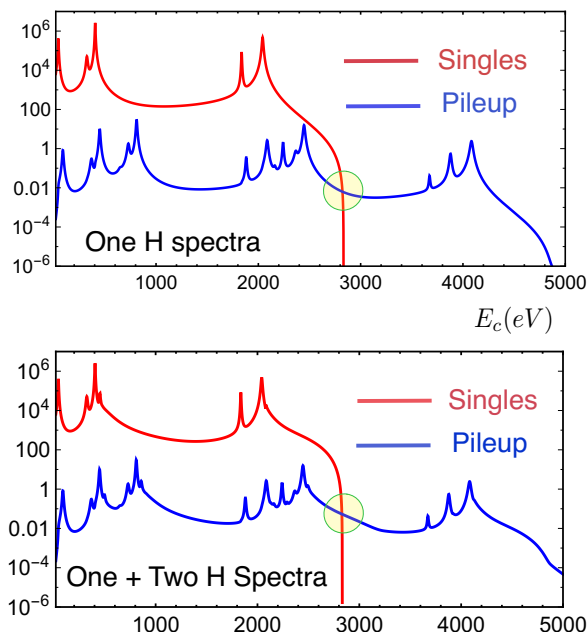
Figure 12. "Singles" and "Pileup" spectral shapes, with a 4×10^{-5} pileup probability and an arbitrary (but common) vertical scale normalization. *Above*: spectra with captures resulting only in single holes. *Below*: spectra with the addition of events resulting in double holes. The regions around $E_c = Q$ are significantly different in the upper and lower plots.

$E_c \sim Q$ domains, which we do in figure 13. The ratio of single to pileup events at, for instance, $E_c = Q - 3\,\text{eV}$ is ~ 6 times larger in the lower part of this figure (where two-hole effects are included) than in the upper part (where they are not).

The reason why we find improved expectations concerning pileup is simple. At $E_c \sim Q$ the pileup spectrum is dominated by the addition of the N1H{c,o} and M1H{c,o} spectral tails, while the singles spectrum is dominated by the latter. But in the pile-up integral of eq. (7.1) all spectral features are partially smoothed out.

8 Single-hole peaks, BW tails and residua

A clear conclusion from the existing data is that there are spectral contributions not anticipated in a simple single-hole theory. In the current exploratory phase of the experiments it would be tempting to subtract from the data the single-hole expectation, to visualize directly the *residuum*: the cited extra contributions. One could, for instance, subtract the blue curve in figure 4 from the black one, to extract the red one: the residual sum of double-hole contributions. We now address the question of the precision with which this can be done.

Given the large statistics with which single-hole contributions will be measured at and around their peaks, there is no question that their individual parameters (position, height and width) will be exquisitely measured. But to obtain the residua a BW shape in eqs. (3.1), (3.2), extending up to very many widths above the peak, must be assumed.
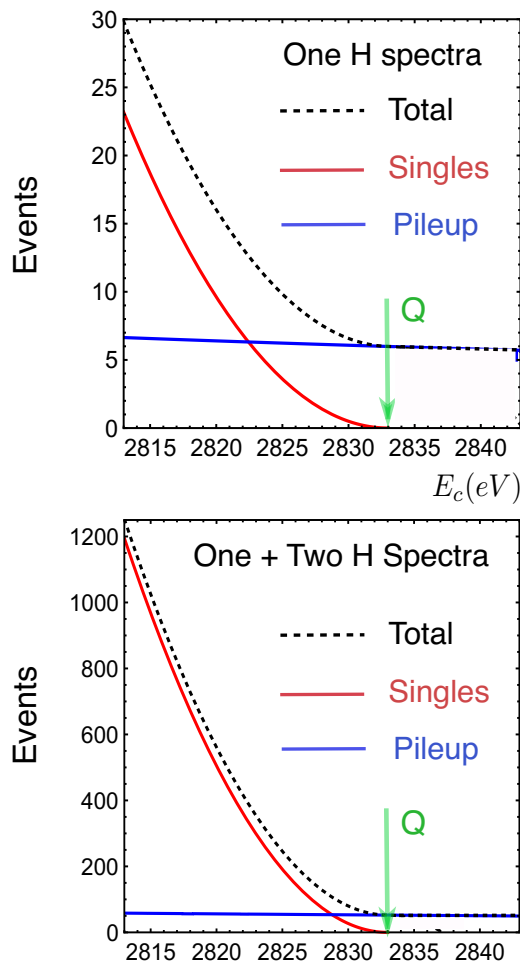
Figure 13. Blowup of the domains $Q - 20\,\mathrm{eV} < E_c < Q + 10\,\mathrm{eV}$ of figure 12. *Above*: spectrum dominated by single holes. *Below*: with the addition of two-hole processes. The vertical scales of the two plots correspond to the same assumed activity of the source and data-taking time.

A Breit-Wigner is an approximation known to require, in certain cases, potentially large explicit corrections [30].

The proof that in the calorimetric case at hand the simple standard BW shape we have used is perfectly well suited is lengthy. We relegate it to appendix B.

9 The shortcomings of theory

The precise treatment of a process in an atom with 67 electrons is obviously intricate. One limitation, in the case of EC, is the use of the sudden approximation. While it is justified in the analysis of electrons captured from the inner orbitals, it is less so for captures from the $n \geq 3$ levels of interest here.

In the sudden approximation (e.g. in a β-decay) and in estimating secondary-hole probabilities, the time required for the change of nuclear charge is assumed to be negligible relative to the typical atomic orbital times: the time it takes them to "react" to the new

environment. In EC this assumption — used for decades without hardly a comment — is extended to the comparison of the time required to propagate the information that the captured electron has disappeared, relative to the rest of the characteristic atomic times: the former must be negligible.

The opposite to the sudden extreme is the adiabatic case, in which the electronic orbitals have time aplenty to slowly evolve from the parent-atom eigenstates to the daughter-atom ones. In the extreme adiabatic limit the probability of making "second holes" would vanish.

9.1 The nuclear capture time

The characteristic time, τ_N, for the EC process $p + e \rightarrow n + \nu$ underlying the nuclear transition is the inverse of the energy transfer q_0. For a process with Q $\ll m_e$, such as the one under discussion, $q_0 \simeq m_e$ and $\tau_N \simeq 1/q_0$ is orders of magnitude smaller than any characteristic atomic time. In the nuclear sense, EC is instantaneous.

9.2 Our two-electron approach

In the simple approach that we have discussed in section 3, two electrons (the captured one and the one that is potentially exiting its orbital) play a singular role. The rest of the electrons are only there to imply some effective values of Z or to forbid some transitions. But once more, a non-relativistic Coulombic approximation[8] provides guidance, which in the case of the adequacy of the sudden approximation turns out to be quite relevant.

The relativistic retardation of signals implies that the sudden nuclear transition $Z \rightarrow Z - 1$ cannot be instantaneously felt by an electron in an orbital of mean radius r. It takes a time of order r for the orbital to be "informed". Similarly, the absence of the electron that was captured is felt by another atomic electron after a time of the order of the larger of the two mean orbital radii.

Recall that the mean radius and binding energy of a Coulombic eigenfunction, in the usual notation, are:

$$r[n, l] = [3\, n^2 - l(l + 1)]/(2\, m_e\, Z\, \alpha) \tag{9.1}$$

$$E[n] = m_e\, (Z\, \alpha)^2/(2\, n^2) \tag{9.2}$$

The quantum-mechanical characteristic time for a bound state to "react" to a perturbation is the inverse of its binding energy. Thus, deviations from the sudden approximation in a transition amplitude are, up to a factor of $\mathcal{O}(1)$, governed by a figure of merit δ, the ratio of the "retardation" time to the quantum-mechanical "reaction" time:

$$\delta \sim E \times r = \mathcal{O}(Z\, \alpha) \tag{9.3}$$

For $\delta \ll 1$ the sudden approximation is justified, while $\delta \gg 1$ corresponds to the adiabatic limit.

---

[8]We used the limit $v/c \rightarrow 0$ everywhere but in allowing for the particularly large effect of EC from the $l = 1$, $j = 1/2$ orbitals.

In numerical examples, let us use the radius of an $l = 0$ orbital as a characteristic light-travel time, $t = r[n, 0]$. The "retardation time" for another S-wave orbital, n', to be informed that the capture process has taken place is of order $t_r = \max(t[n], t[n'])$, so that $\delta = E[n'] \, t_r$.

For an M1 capture and a putative second hole in N1, $\delta = 3Z\alpha/4$, that is a worrisome $\delta = 0.24$ for $Z_{\text{eff}} = 43.2$. But for the energies and mean radii obtained in a non-relativistic Hartree-Fock calculation, $E(\text{N1}, \text{Ho}) = 0.414 \, \text{keV}$, $\langle r(\text{N1}, \text{Ho}) \rangle = 0.29 \, \text{Å}$, and $E \times r \sim 0.062$, a much smaller result. After a brief scare, the sudden approximation appears once again to be justified.

In our two-active-electron approach the use of (suddenly) overlapping wave-function is safe, but the wave functions themselves are crude approximations. Thus the potential interest of more ambitious calculations.

9.3 A many electron system

The methods of Faessler and collaborators [17–19] are relativistic,[9] and consistently use Slater determinants to describe the fully anti-symmetrized states of the Ho and Dy* atoms. In each atom the individual orbitals span an orthonormal set. For Dy* this implies that *all* of its electrons must have had ample time, after the nuclear capture, to readjust to the new situation.

Consider the capture of an M1 electron; the mean radius of its orbital is $\langle r(\text{M1}, \text{Ho}) \rangle = 0.13 \, \text{Å}$, which we will take as the pertinent time for the capture information to arrive to three inner orbitals. For the other electron in the M1 state, whose binding energy is $E(\text{M1}, \text{Ho}) = 2.05 \, \text{keV}$, the figure of merit is $\delta = E(\text{M1}) \, r(\text{M1}) \sim 0.135$. For an L1 electron, $E(\text{L1}, \text{Ho}) = 9.05 \, \text{keV}$ and $\delta = E(\text{L1}) \, r(\text{M1}) \sim 0.6$. Finally, for a K electron $E(\text{K}, \text{Ho}) = 55.6 \, \text{keV}$, and $\delta = E(\text{K}) \, r(\text{M1}) \sim 3.7 > 1$.

We conclude that the sudden approximation is not good for the Dy* atom in its ensemble. This statement is very specific to cases in which the captured electron belongs to a rather external orbit: M1 or higher in the case of ^{163}Ho. Should we have discussed K-capture, the characteristic radius (or time) to spread the information would have been a K radius and the energies of the orbits in which second holes may be produced a K binding energy, or a smaller one. The sudden-approximation figure of merit, δ, would have always been significantly smaller than unity, justifying the sudden approximation.

10 Platinum

We have only discussed ^{163}Ho. But measurements of the next-to-best electron-capturing isotope [5], ^{193}Pt, could be of help in understanding the difficult theoretical issues associated with the two-hole contributions. The problem is simply one of QED, like in the case of holmium or the slightly harder problem of understanding the human brain.

---

[9]The corrections to a non-relativistic approach are of $\mathcal{O}(Z\alpha)$, like the effects neglected by use of the sudden approximation.

11 Conclusions

The current very preliminary data on the calorimetric spectrum of ^{163}Ho decay, in the region of the N peaks, appear to be qualitatively described by the simplified theory we have discussed. A similarly preliminary conclusion is that the description of the observations becomes quantitively satisfactory when the various theoretical single- and double-hole features are renormalized to fit the data. Once the data improve, we expect this conclusion to become more solid.

On the way to measure or limit the neutrino mass, the relevant energy domain is not yet explored. It is the one extending from the M2 and M1 single peaks towards the spectral endpoint, the interval we have analized in detail. It is there that future data and the comparison of its features with theory will be of utmost interest.

We argued that, relative to the "old theory" with only single-hole contributions, double-hole effects may enhance the spectral endpoint region by a factor of ~ 40. If this is correct, the statistical sensitivity on m_ν — which varies as the fourth root of the number of decays — would improve by a factor ~ 2.5. We showed that the pileup problem would also be reduced by an even larger factor.

We cannot indubitably trust the above optimistic conclusions. Thus, we have also studied the possibility that double- and single-hole contributions be of similar magnitude close to the endpoint. This choice makes the theoretical analysis of the data more challenging. But we have argued that also in this very pessimistic case the introduction of just one extra parameter — besides m_ν, Q and the slope of a linear function of E_c — should be enough to analyse the data along well-trodden paths.

An issue that remains to be investigated is the possible existence, in a given calorimeter's substrate, of BEFS oscillations. These would be due to Ho-decay electrons undergoing reflections in the crystal lattice [31, 32].

The possibility of a significant contribution of electron shake-ups, leading to double-hole spectral peaks, was originally presented as very damning [12, 13]. Somewhat ironically, the likely existence of a significant contribution of electron shake-offs may be a very welcome blessing.

A Interferences

In the single-hole spectrum of eq. (3.1) quantum interferences have been omitted. To discuss how good an approximation this is, we concentrate on the potentially most significant interference: the one between the M1 and N1 amplitudes. For them to interfere, the
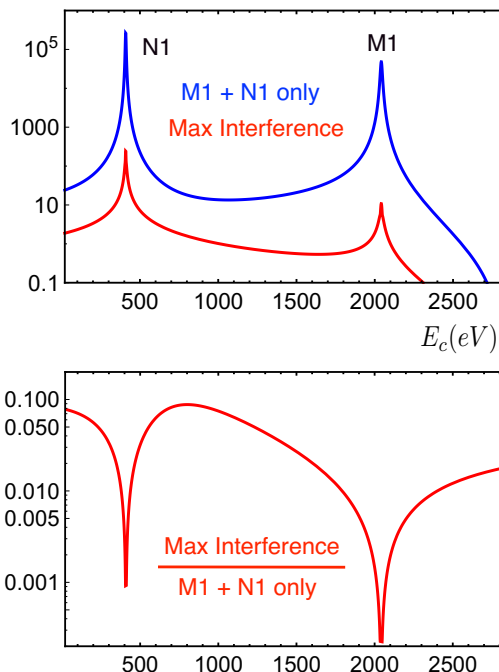
Figure 14. Generous upper limits to the absolute value of the M1-N1 interferences, for a hypothetical spectrum with only single M1 and N1 captures. *Above*: the spectrum and the maximum interference. *Below*: the ratio of the maximum interference term to the non-interfering spectrum.

$j = \mathrm{M1}, \mathrm{N1}$ holes must decay into the same (generally two-hole) final state f. Introduce the notation by writing the corresponding amplitude and probability as:

$$A_j^f \propto \phi_j(0) \, \frac{\sqrt{\gamma_j/\pi}}{E - E_j + i\,\gamma_j} \sqrt{b(j \to f)} \; e^{i\psi_j^f} \;, \tag{A.1}$$

$$\Gamma^f \propto \left| \sum_j A_j^f \right|^2 = \sum_j |A_j^f|^2 \; + \; \sum_{k \neq j} A_k^f \, (A_j^f)^* \;, \tag{A.2}$$

where $\gamma_j \equiv \Gamma_j/2$ is the half-width, $b(j \to f)$ is the branching fraction for this decay and ψ_j^f is the unknown phase. Summing over all possible f in eq. (A.2), the first (second) term is the single hole expression (the interference). The explicit expression for the latter is:

$$2\,\phi_M(0)\phi_N(0)\frac{\sqrt{\gamma_M \gamma_N}}{\pi}\beta \tag{A.3}$$

$$\times \frac{[(E - E_M)(E - E_N) + \gamma_M \gamma_N]\cos(\psi) + [\gamma_M(E - E_N) - \gamma_N(E - E_M)]\sin(\psi)}{[(E - E_M)^2 + \gamma_M^2]\,[(E - E_N)^2 + \gamma_N^2]} \;,$$

where we have suppressed the c in E_c, the 1 in M1 and N1, β stands for $\sum_f \sqrt{b(M \to f)\,b(N \to f)}$ and ψ is the residual unknown phase.

In searching for an upper limit to the interference term, we substitute β by the larger number $[\sum_f b(M \to f) \times \sum_f b(N \to f)]^{1/2} \sim 0.088$, where the numerical value is from [27, 28]. Moreover, in eq. (A.3) we take either $\cos(\psi)$ or $\sin(\psi)$ to be unity, depending on which of the two, at a given E, has the coefficient with the largest absolute value. The results of

eqs. (A.2), (A.3) are used to draw figure 14, in whose lower panel we see that $\sim 2\%$ would be a generous upper limit for the fractional contribution of the interference term close to the endpoint.

The conclusion is that interferences can be neglected in the endpoint analysis, more so if two-hole effects are dominant there.

B The tails of resonances

In writing, in the usual fashion, the contribution to the calorimetric spectrum of a given hole of (positive) binding energy E_H, we have first employed the negligible-width approximation and the two-body phase space, dN_2, for the process $Ho \to Dy^* + \nu$ to write:

$$dN_2/dE_\nu \propto p_\nu\, \delta(E_\nu - Q + E_H)\, E_\nu, \tag{B.1}$$

where the square of the capture matrix element is $\propto E_\nu$. Since in this case $E_c = E_H$ one simply has:

$$\frac{dN_2}{dE_c} \propto \sqrt{(Q - E_c)^2 - m_\nu^2}\, \delta(E_c - E_H)\,(Q - E_c) \tag{B.2}$$

The contribution of a hole of non-zero width Γ_H can then be obtained by substituting the δ function by a BW to get, for the sum of single-hole contributions, eqs. (3.1)–(3.3).

The purpose of the above naive reminder is to discuss the extent to which eq. (3.2) is a good approximation, specially very many widths above a given resonance, in particular the one corresponding to an M1 hole, whose contribution dominates the end of the spectrum. In this respect, two related items need to be discussed, both concerning the single-hole contributions to the calorimetric spectrum. The first is whether or not the two-body phase space is the correct one to use, in spite of the fact that Dy* may decay to its ground state by photon emission, in which case the process appears to have one extra final-state body (the photon). More often, the Dy* de-excitation starts with a complicated chain of electron emissions, an apparently many-body final state. In all cases the question arises: is the two-body Breit-Wigner shape of eqs. (3.1), (3.2) adequate far away from its peak?

Consider, as a "sanity test", the possible but relatively very improbable case in which the hole made by EC in the neutral daughter atom, Dy*, decays to the Dy ground state by having the Dy* outermost electron transit to the hole, with the emission of a photon. This is a process in which $E_c = E_\gamma$, and its phase space, dN_3, is a three-body one: $Ho \to Dy + \nu + \gamma$. Relative to eq. (B.2), the calorimetric spectrum acquires two extra factors:

$$dN_3/dE_c \propto E_c\, |M_\gamma|^2\, dN_2/dE_c, \tag{B.3}$$

where $E_c = E_\gamma$ arises from the photon's phase-space and M_γ is the photon emission matrix element.

The E_c dependence in eqs. (3.2) differs from that in eq. (B.3). This is a well known situation [30], generally "remedied" by "incorporating" the kinematics (the extra factor of E_c) or the kinematics and dynamics ($E_c\, |M_\gamma|^2$) into an effective width.

Suppose we adopt the first of the two mentioned remedies by substituting

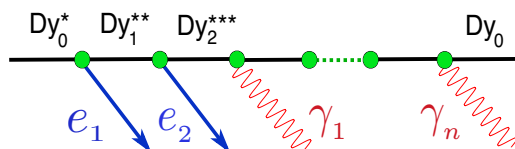$$\Gamma_H \to \widetilde{\Gamma}_H = \Gamma_H\, E_c/E_H. \tag{B.4}$$

Figure 15. A dominant chain of decays in the process $Ho \to \nu + Dy^*$; $Dy^* \to e's \& \gamma's + Dy_0$, with Dy_0 the ground state of dysprosium. The subscripts of Dy are electric charges and the stars the number of holes.

Take the example of M1 capture ($E_{M1} \simeq 2048\,eV$). The modification of the width in the denominator of the BW expression is immaterial at the endpoint, for $(Q - E_{M1})^2 \gg \widetilde{\Gamma}_{M1}^2/4$. But the modification of the width in the numerator would alter the naive result from eq. (3.2) by a factor changing linearly from 1 at $E_c = E_{M1}$ to $Q/E_{M1} \simeq 1.37$ at $E_c = Q$. This seems to be worrisome.

As it turns out, in the specific case at hand, the traditional expression naively based on two-body phase space considerations, eqs. (3.1), (3.2), is the correct one to use. One reason is that the single-photon Dy* decay we discussed — which would require a three-body phase space treatment — has a negligible branching ratio. The dominant decays consist of a series of Auger or Coster-Kronig transitions (in which the neutral Dy* emits electrons, becoming an increasingly charged ion), followed by radiative transitions in which an outer atomic electron — or one coming from the negatively charged atomic neighborhood — drops into the Dy-ion holes and a photon is emitted. These processes are depicted in figure 15.

Consider any of the electron emissions in figure 15. The corresponding phase space expression contains a factor p_e, the momentum of the outgoing electron. But, at the relevant very non-relativistic energies, this factor, to a very good approximation, is compensated by the "Fermi-function", $F \sim 1/p_e$, which reflects the fact that the wave function of the outgoing electron is not that of a free particle, but the one of an electron subject to the field of a charged ion. For any of the soft photon emissions in figure 15 the pertinent width may be modified by a remedial factor $E_\gamma/\langle E_\gamma \rangle$, but that function differs very little from unity in its narrow allowed range (unless $E_\gamma^{max} \sim Q$, the unlikely case discussed in the next paragraph).

The emission of only one photon is highly suppressed, as we said above. There still remains the possibility that one of the (many) photons emitted in the decay — as depicted in figure 15 — carries all of the energy $E_c \simeq Q$, requiring a modified width in the corresponding Breit-Wigner. But in that case all the other emitted photons have momenta $p \simeq 0$ and the phase space (multiply) vanishes. The multi-body phase space has a multidimensional pole at the central energies of each of the transitions. At $E_c \simeq Q$ the overwhelmingly most likely situation corresponds to all energies being close to this multiple pole and adding up to $E_c \simeq Q$. All in all the overall process is described by the naive two-body phase space expression of eq. (3.2), with its width unmodified.

To conclude: an event in the process we are discussing can be viewed as the two-body decay of the calorimeter "before" to a neutrino and the unstable "excited calorimeter" immediately after. The calorimeter then releases its excess energy — which is calorimetrically recorded – to return to a new ground state (with one fewer Ho and one extra Dy atoms).

References

[1] E. Fermi, *An attempt of a theory of beta radiation*, *Nature*, Rejected.

[2] E. Fermi, *Tentativo di una teoria dei raggi beta*, *Nuov. Cim.* **11** (1934) 1.

[3] E. Fermi, *Versuch einer Theorie der Beta-Strahlen*, *Z. Phys.* **88** (1934) 161 [INSPIRE].

[4] G. Drexlin et al., *Current direct neutrino mass experiments*, *Adv. High Energy Phys.* (2013) 293986 [arXiv:1307.0101].

[5] A. De Rújula, *A new way to measure neutrino masses*, *Nucl. Phys.* **B 188** (1981) 414 [INSPIRE].

[6] A. De Rújula and M. Lusignoli, *Calorimetric measurements of ^{163}Ho decay as tools to determine the electron neutrino mass*, *Phys. Lett.* **B 118** (1982) 429 [INSPIRE].

[7] A. Nucciotti, *The use of low temperature detectors for direct measurements of the mass of the electron neutrino*, arXiv:1511.00968 [INSPIRE].

[8] P.C.-O. Ranitzsch et al., *Development of metallic magnetic calorimeters for high precision measurements of calorimetric ^{187}Re and ^{163}Ho spectra*, *J. Low Temp. Phys.* **167** (2012) 1004.

[9] L. Gastaldo et al., *The electron capture ^{163}Ho experiment ECHo*, *J. Low Temp. Phys.* **176** (2014) 876.

[10] B. Alpert et al., *HOLMES — The Electron Capture Decay of ^{163}Ho to measure the electron neutrino mass with sub-eV sensitivity*, *Eur. Phys. J.* **C 75** (2015) 112 [arXiv:1412.5060] [INSPIRE].

[11] M.P. Croce et al., *Development of holmium-163 electron-capture spectroscopy with transition-edge sensors*, arXiv:1510.03874 [INSPIRE].

[12] R.G.H. Robertson, *Can neutrino mass be measured in low-energy electron capture decay?*, arXiv:1411.2906v1.

[13] R.G.H. Robertson, *Examination of the calorimetric spectrum to determine the neutrino mass in low-energy electron capture decay*, *Phys. Rev.* **C 91** (2015) 035504 [arXiv:1411.2906] [INSPIRE].

[14] ECHo collaboration, S. Eliseev et al., *Direct measurement of the mass difference of ^{163}Ho and ^{163}Dy solves the Q-value puzzle for the neutrino mass determination*, *Phys. Rev. Lett.* **115** (2015) 062501 [arXiv:1604.04210] [INSPIRE].

[15] G. Audi, A.H. Wapstra, and C. Thibault, *The Ame2003 atomic mass evaluation (II). Tables, graphs and references*, *Nucl. Phys.* **A 729** (2003) 337 [INSPIRE].

[16] ECHo collaboration, C. Hassel et al., *Recent results for the ECHo experiment*, *J. Low Temp. Phys.*, to be published.

[17] A. Faessler, L. Gastaldo and F. Simkovic, *Electron capture in ^{163}Ho, overlap plus exchange corrections and neutrino mass*, *J. Phys.* **G 42** (2015) 015108 [arXiv:1407.6504] [INSPIRE].

[18] A. Faessler and F. Simkovic, *Improved description of one- and two-hole states after electron capture in* ^{163}Ho *and the determination of the neutrino mass*, *Phys. Rev.* **C 91** (2015) 045505 [arXiv:1501.04338] [ɪɴSPIRE].

[19] A. Faessler, C. Enss, L. Gastaldo and F. Šimkovic, *Determination of the neutrino mass by electron capture in* ^{163}Ho *and the role of the three-hole states in* ^{163}Dy, *Phys. Rev.* **C 91** (2015) 064302 [arXiv:1503.02282] [ɪɴSPIRE].

[20] W. Bambynek et al., *Orbital electron capture by the nucleus*, *Rev. Mod. Phys.* **49** (1977) 77 [*Erratum ibid.* **49** (1977) 961] [ɪɴSPIRE].

[21] A. De Rújula and M. Lusignoli, *The calorimetric spectrum of the electron-capture decay of* ^{163}Ho. *A preliminary analysis of the preliminary data*, arXiv:1510.05462 [ɪɴSPIRE].

[22] M. Nakagawa, H. Okonogi, S. Sakata and A. Toyoda, *Possible existence of a neutrino with mass and partial conservation of muon charge*, *Prog. Theor. Phys.* **30** (1963) 727 [ɪɴSPIRE].

[23] R.R. Shrock, *New tests for and bounds on neutrino masses and lepton mixing*, *Phys. Lett.* **96B** (1980) 159.

[24] R.L. Intemann and L. Pollock, *K-electron ejection accompanying nuclear K capture*, *Phys. Rev.* **157** (1967) 41.

[25] L.D. Landau and E.M. Lifchitz, *Mécanique quantique*, MIR, Moscow, Russia (1974), see par. 36.

[26] A.D. MacLean and R.S. McLean, *Roothaan-Hartree-Fock atomic wave functions Slater basis-set expansions for* $Z = 55$-92, *Atom. Data Nucl. Data Tables* **26** (1981) 197.

[27] E.J. McGuire, *M-shell Auger, Coster-Kronig, and radiative matrix elements, and Auger and Coster-Kronig transition rates in j-j coupling*, Sandia Laboratories Report SC-RR-71-0835 (1972).

[28] E.J. McGuire, *N-shell Auger, Coster-Kronig, and radiative matrix elements, and Auger and Coster-Kronig transition rates in j-j coupling*, Sandia Laboratories Report SAND-75-0443 (1975).

[29] M. Lusignoli and M. Vignati, *Relic antineutrino capture on* ^{163}Ho *decaying nuclei*, *Phys. Lett.* **B 697** (2011) 11 [*Erratum ibid.* **B 701** (2011) 673] [arXiv:1012.0760] [ɪɴSPIRE].

[30] Particle Data Group, K.A. Olive et al., *Review of particle physics*, *Chin. Phys.* **C 38** (2014) 090001.

[31] S.E. Koonin, *Environmental fine structure in low-energy beta-particle spectra*, *Nature* **354** (1991) 468.

[32] F. Gatti et al., *Detection of environmental fine structure in the low-energy beta-decay spectrum of* ^{187}Re, *Nature* **397** (1999) 137.